Optical Properties of Strained-Layer Superlattices with Growth Axis along [111]

D. L. Smith
Los Alamos National Laboratory, Los Alamos, New Mexico 87545

and

C. Mailhiot
Xerox Webster Research Center, Webster, New York 14580
(Received 8 December 1986)

We show that large piezoelectrically induced electric fields strongly modify the optical properties of strained-layer superlattices with growth axis along [111]. These internal fields reduce the superlattice band gap, change optical matrix elements, and cause a spatial separation of photoexcited electrons and holes so as to screen the fields. Very large ($\chi^3 \sim 10^{-1}$ esu) optical nonlinearities occur because of the free-carrier screening of the strain-generated internal electric fields.

PACS numbers: 73.40.Kp, 73.40.Lq, 78.40.Fy

It is now well established that strained-layer superlattices, that is, superlattices whose constituent materials have somewhat different lattice constants, can be grown with a high degree of crystalline perfection.[1-3] For sufficiently thin layers, the lattice-constant mismatch is accommodated by internal strains rather than by the formation of dislocations. The internal strains generated by the lattice-constant mismatch can be rather large and can substantially change the electronic structure of the strained-layer superlattices.[4] Recently, a new effect in strained-layer superlattices with a [111] growth axis has been predicted: large internal electric fields generated by the piezoelectric effect.[5] In this Letter, we show that these internal fields can strongly modify the optical properties of the superlattice, and because the internal fields are screened by photogenerated carriers, they can lead to very strong optical nonlinearities.

Group III-V and group II-VI semiconductors are piezoelectric. Thus, strains in these materials can lead to electric polarization fields. For strained-layer superlattices with a [111] growth axis, the orientation of the lattice-constant mismatch-induced strains is such that polarization fields directed along the growth axis are generated.[5,6] Because one of the constituent materials is in biaxial compression and the other is in biaxial tension, the signs of the electric polarization vectors are opposite in the two constituent materials. Thus, there is a nonzero divergence of polarization (a polarization charge) at the superlattice interfaces. These polarization charges generate internal electric fields directed along the growth axis and having opposite polarities in the two constituent materials.[7] The magnitude of the electric fields can be very large, exceeding 10^5 V/cm, for lattice-constant mismatches of the order of 1%.[5]

The strain-induced electric field can significantly change the electronic structure and the optical properties of the superlattice. We consider superlattices made from $Ga_{0.47}In_{0.53}As$-$Al_{0.70}In_{0.30}As$, with the Ga containing alloy layers half as thick as the Al-alloy layers. This is a type-I superlattice in which the smaller-band-gap (quantum well) Ga alloy is in biaxial compression. The lattice-constant mismatch is 1.5%. The strain-induced electric field is 1.4×10^5 V/cm in the Ga alloy and half this value in the Al alloy.[8] We use the approach described earlier[9] for the electronic structure calculations. The internal electric fields are included as in Mailhiot and Smith.[10] Input parameters to the calculations (valence-band off sets, deformation potential parameters, etc.) are chosen as described in these references.

Both electronic energy levels and wave functions are changed by the internal electric fields.[11] The changes in the wave functions lead to changes in optical matrix elements and to a screening of the electric fields by photogenerated electron-hole pairs. In Fig. 1, we show the effect of the electric fields on electronic energy levels, optical matrix elements, and the dipole moment of an electron-hole pair. Figure 1(a) shows the zone-center energy levels of the lowest conduction band and the highest three heavy-hole and highest light-hole energy levels as functions of the superlattice repeat distance (keeping the well-to-barrier length ratio fixed) with inclusion and neglect of the electric fields. The fields shift the conduction-band state to lower energy and the valence band to higher energy, thus reducing the band gap. The effect is larger for thicker-layer superlattices, and at a given thickness if larger for the heavy holes than for the electrons or the light holes. The light-hole bands are split away from the heavy-hole bands by strain. Therefore, band-edge optical properties will be dominated by heavy-hole–to–conduction-band transitions.

In Fig. 1(b), we show the squared optical matrix elements, defined as

$$|M|^2=\sum_{ii'}(2/m)\,|\langle n_i|\mathbf{p}\cdot\hat{\boldsymbol{\varepsilon}}|n_{i'}\rangle|^2,$$

for the first three heavy-hole–to–conduction-band transitions (labeled hh_j-C_1) as functions of the internal elec-

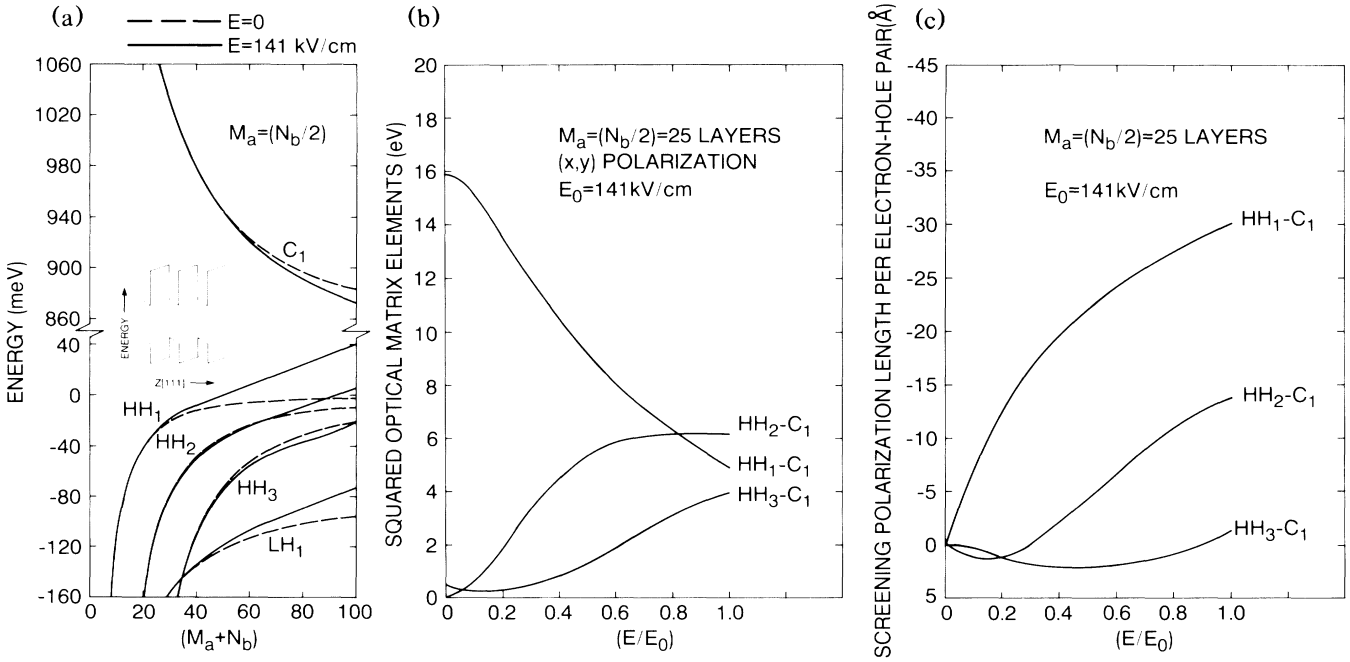

FIG. 1. (a) Superlattice energy levels as functions of repeat distance with (solid line) and without (dashed line) the internal fields. (b) Squared optical matrix elements and (c) electron-hole pair dipole screening length as functions of the internal field strength for the 25/50 superlattices.

tric field in the Ga alloy. Here $|n_i\rangle$ are superlattice zone-center eigenstates, the sums on i are over the degenerate pairs of eigenstates, and $\hat{\boldsymbol{\varepsilon}}$ is a unit polarization vector. The superlattice consists of 25 molecular layers of the Ga alloy alternated with 50 molecular layers of the Al alloy. (We refer to this as a 25/50 superlattice.) The polarization is in the plane of the superlattice interfaces. The maximum field shown (E_0) is the unscreened value of the strain-induced field. The hh_1-C_1 transition, which is strongly allowed at zero field, is suppressed by the internal fields. The hh_2-C_1 and hh_3-C_1 transitions are very weak at zero field. The internal fields increase the strength of these transitions so that, at the unscreened value of the fields, the three transitions have comparable oscillator strength.

In Fig. 1(c) we show the screening polarization length of an electron-hole pair, defined as

$$I_{nn'}(E)=\int_{-a}^{0} dz\,(z+a/2)[C_n(z)-C_{n'}(z)],$$

for hh_j-C_1 ($j=1,3$) electron-hole pair states as a function of the internal field in the Ga alloy. Here, the integral extends along the growth axis across one quantum well, n (n') labels hole (electron) states, and $C_n(z)$ $[-C_{n'}(z)]$ is the coarse-grain averaged hole (electron) charge density. This screening length is the length of the dipole moment of an electron-hole pair in the indicated quantum states and electric field. The negative sign in Fig. 1(c) indicates a dipole moment that opposes the strain-generated internal field. The screened field in the quantum well is given by

$$E[1-P(E)/\varepsilon_0\varepsilon E]=E_0,$$

where

$$P(E)=N[(a+b)/a]eI(E),$$

and a is the quantum well thickness, b is the barrier thickness, N is the density of electron-hole pairs, and ε is the static dielectric constant in the quantum well. To reduce the unscreened internal field by 10% for the superlattice requires a density of 1.2×10^{17}-cm^{-3} electron-hole pairs (holes in hh_1 state). The screening is predominantly from distortion of the hole wave function.

Because the internal electric fields change the superlattice energy levels and wave functions, they change the superlattice optical properties. We consider the 25/50 superlattice and present calculations of the resonant contribution to the susceptibility from near-band-edge transitions. Transitions from the first three heavy-hole bands in the lowest conduction band are included. [Transitions from the light-hole bands occur at higher energy; see Fig. 1(a).] The effects of the internal electric fields on the exciton binding energies and wave functions are included, but they are rather small.[12] A scattering time (T_2), which gives a FWHM of 5 meV, is included.

In Fig. 2, we show the calculated real and imaginary parts of the resonant susceptibility as functions of photon energy for three values of the internal fields: the unscreened value, half the unscreened value, and zero field.

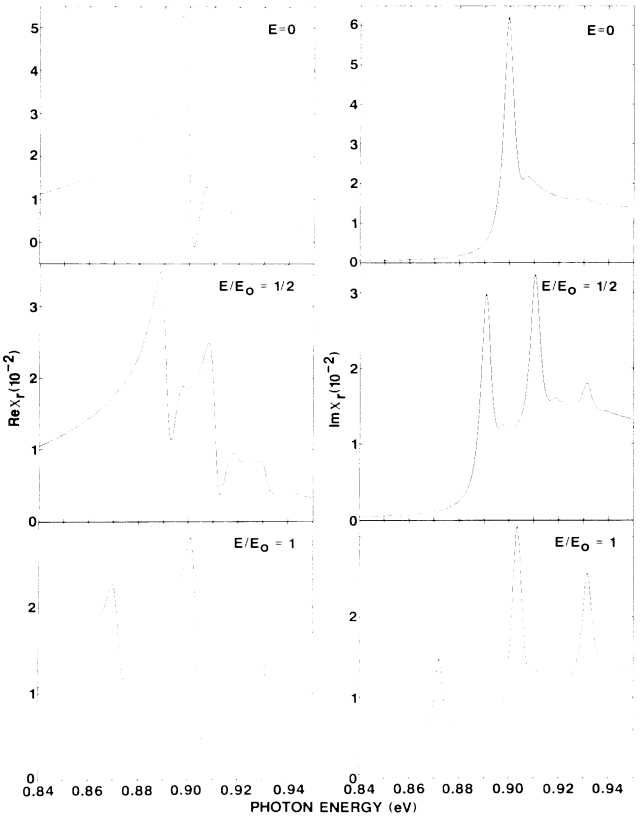

FIG. 2. Real part (left) and imaginary part (right) of the resonant susceptibility as functions of photon energy for three values of the internal field for the 25/50 superlattice.

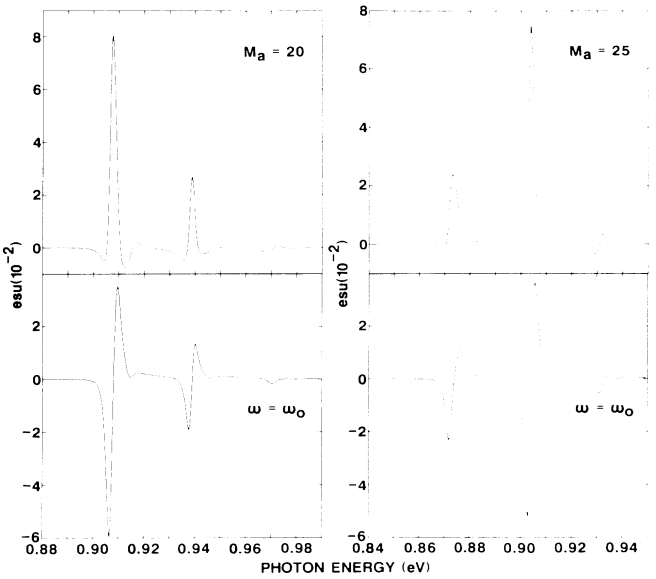

FIG. 3. Real part (top) and imaginary part (bottom) of $\chi^{(3)}$ as functions of photon energy for equal pump (ω_0) and probe (ω) frequencies; 20/40 (left) and 25/50 (right) superlattices.

At zero field, hh_1-C_1 transitions dominate the spectrum; there is a strong exciton transition and an electron-hole continuum. A small hh_3-C_1 exciton transition is superposed on the hh_1-C_1 continuum. The hh_2-C_1 transitions are too weak to show up. As the internal fields increase, the hh_1-C_1 exciton moves to lower energy and loses oscillator strength. With increasing field, the hh_2-C_1 transitions are turned on. At the unscreened value of the fields, the hh_2-C_1 exciton is the strongest feature in the spectrum. It moves to lower energy with increasing field, but at a slower rate than the hh_1-C_1 exciton does. The hh_3-C_1 exciton gains oscillator strength with increasing field and moves to slightly higher energy.

As seen in Fig. 2, the internal, strain-generated electric fields can significantly change the optical properties of a superlattice. These internal fields can be externally modulated. Here we consider modulation of these fields by across-band-gap optical absorption. The electron-hole pairs formed by this absorption process screen, and thus reduce, the magnitude of the internal fields. This screening effect gives the superlattice nonlinear optical properties. The size of the optical nonlinearity can be determined by our calculating the susceptibility at two slightly different values of the internal fields and finding the carrier density and, hence, the absorbed intensity required to cause that shift in the internal electric fields. The holes will rapidly thermalize to the hh_1 band independent of where they were optically generated. Thus, we take the screening to be caused by hh_1-C_1 electron-hole pairs. We use a value of 10 ns for the electron-hole pair lifetime. The initial electric field is taken as the unscreened value.

In Fig. 3, we show real and imaginary parts of the nonlinear susceptibility at a single frequency $\chi^{(3)}(-\omega;\omega,\omega,-\omega)$,[13] as a function of frequency for a 20/40 and a 25/50 superlattice. Very strong features ($\sim 10^{-1}$ esu) occur near the hh_1-C_1 and hh_2-C_1 exciton transitions. Comparing line shapes in Fig. 3 (peak in Re$\chi^{(3)}$, derivative of peak in Im$\chi^{(3)}$) with Fig. 2, one sees that these features in $\chi^{(3)}$ result primarily from shifting the exciton transition energy. The hh_2-C_1 nonlinearity is stronger than the hh_1-C_1 nonlinearity in the 25/50 superlattice, whereas the reverse is true for the 20/40 superlattice. This reversal occurs because the internal fields have caused the hh_2-C_1 oscillator strength to exceed the hh_1-C_1 oscillator strength at the unscreened value of the fields in the 25/50 superlattice. In the 20/40 superlattice the hh_1-C_1 oscillator strength is larger at the unscreened fields. A smaller feature in $\chi^{(3)}$ occurs near the hh_3-C_1 transition. From the line shape one sees that this nonlinearity results primarily from the exciton oscillator strength's changing with field.

In summary, we have shown that internal electric fields generated by strain in strained-layer superlattices with growth axis along [100] significantly change the op-

tical properties of the superlattice. We specifically considered across-band-gap optical transitions in type-I superlattices and found that the strain-induced fields reduce the band gap and turn on normally weak transitions. We have shown that the magnitude of the strain-induced fields can be externally modulated by photoabsorption. We found that this modulation leads to very large optical nonlinearities ($\chi^{(3)} \sim 10^{-1}$ esu). The magnitude of these nonlinearities is comparable to optical nonlinearities observed from exciton saturation,[14] although the physical processes involved in the two mechanisms are quite different.[15]

The work of one of us (D.L.S.) has been financially supported by Los Alamos National Laboratory Internal Supporting Research.

[1]J. W. Matthews and A. E. Blakeslee, J. Cryst. Growth **27**, 118 (1974), and **29**, 273 (1975), and **32**, 265 (1976).

[2]G. C. Osbourn, R. M. Biefield, and P. L. Gourley, Appl. Phys. Lett. **41**, 172 (1982).

[3]I. J. Fritz, L. R. Dawson, and T. E. Zipperian, Appl. Phys. Lett. **43**, 846 (1983).

[4]G. C. Osbourn, J. Appl. Phys. **53**, 1586 (1982).

[5]D. L. Smith, Solid State Commun. **57**, 919 (1986).

[6]For strained-layer superlattices with growth axis along [100], no polarization fields are generated.

[7]Because the electric field changes polarity in the two constituent materials, the case discussed here is different from the application of an external electric field to a superlattice.

[8]Surface charge accumulation will eliminate the potential drop across the superlattice. Thus, the integral of the electric field over a superlattice period will vanish.

[9]D. L. Smith and C. Mailhiot, Phys. Rev. B **33**, 8345 (1986); C. Mailhiot and D. L. Smith, Phys. Rev. B **33**, 8360 (1986).

[10]C. Mailhiot and D. L. Smith, J. Vac. Sci. Technol. B **4**, 996 (1986).

[11]C. Mailhiot and D. L. Smith, Phys. Rev. B **35**, 1242 (1987).

[12]See, for example, J. A. Brum and G. Bastard, Phys. Rev. B **31**, 3893 (1985).

[13]We define $\chi^{(3)}$ as in S. S. Jha and N. Bloembergen, Phys. Rev. **171**, 891 (1968).

[14]D. S. Chemla, D. A. B. Miller, P. W. Smith, A. C. Gossard, and W. Wiegmann, IEEE J. Quantum Electron. **20**, 265 (1984).

[15]The superlattice system discussed here was not optimized for large optical nonlinearities.